Applied Surface Science 336 (2015) 262–266

Contents lists available at ScienceDirect

Applied Surface Science

journal homepage: www.elsevier.com/locate/apsusc

# Formation of plasmonic colloidal silver for flexible and printed electronics using laser ablation

S. Kassavetis[a,*], S. Kaziannis[b], N. Pliatsikas[a,c], A. Avgeropoulos[a], A.E. Karantzalis[a], C. Kosmidis[b], E. Lidorikis[a], P. Patsalas[c]

[a] University of Ioannina, Department of Materials Science and Engineering, 45110 Ioannina, Greece
[b] University of Ioannina, Department of Physics, 45110 Ioannina, Greece
[c] Aristotle University of Thessaloniki, Department of Physics, 54124 Thessaloniki, Greece

ARTICLE INFO

*Article history:*
Received 15 July 2014
Received in revised form
27 November 2014
Accepted 27 November 2014
Available online 4 December 2014

*Keywords:*
Plasmonic colloidal solutions
Laser ablation
Silver nanoparticles
Organic solvents
Picosecond laser

ABSTRACT

Laser ablation (LA) in liquids has been used for the development of various nanoparticles (NPs); among them, Ag NPs in aqueous solutions (usually produced by nanosecond (ns) LA) have attracted exceptional interest due to its strong plasmonic response. In this work, we present a comprehensive study of the LA of Ag in water, chloroform and toluene, with and without PVP, using a picosecond (ps) Nd:YAG laser and we consider a wide range of LA parameters such as the laser wavelength (1064, 532, 355 nm), the pulse energy (0.3–17 mJ) and the number of pulses. In addition, we consider the use of a secondary nanosecond laser beam for the refinement of the NPs size distribution. The optical properties of the NPs were evaluated by in situ optical transmittance measurements in the UV–vis spectral ranges. The morphology of the NPs and the formation of aggregates were investigated by Scanning Electron Microscopy and High-Resolution Transmission Electron Microscopy.

The ps LA process resulted in the development of bigger Ag NPs, compared to the ns LA, compatible with the size requirements of the printed organic electronics technology. The optimum conditions for the ps LA of Ag in organic solvents include the use of the 355 nm beam at low pulse energy (<1 mJ); these conditions rendered isolated Ag nanoparticles manifesting strong and well defined surface plasmon resonance peak. The use of the secondary ns laser beam was proven to be able to refine the nanoparticles to intermediate size between those produced by the single ns or ps LA.



## 1. Introduction

Organic and printed electronics promise to revolutionize the industries of renewable energy and solid state lighting by the production of large-scale and high-efficiency organic photovoltaics (OPV) and organic light emitting diodes (OLED). Since the original reports about solar cells with increased efficiency due to the incorporation of plasmonic nanoparticles [1–3], great efforts have been dedicated in developing the technologies of plasmon-enhanced OPV [4–9] and OLED [10–12]. Ag is the element that exhibits the stronger plasmonic effects, when in nanoparticle form. Therefore, it is of paramount importance to develop colloidal Ag solutions that would fulfill the requirements of organic and printed electronics, in particular:

(1) The liquid solvent should be compatible with solvents routinely used for printed electronics (e.g. chloroform and toluene are used to print the standard P3HT:PCBM active layer of OPV).
(2) The Ag particle sizes should range from a few nm to some tens of nm to maximize light absorption and scattering, respectively, and preventing the formation of Ag nanoparticles larger than 120–150 nm or micron-scale Ag particles that would short-circuit the OPV or OLED devices, since the thickness of the device individual layers is from 100 to 200 nm.
(3) The Ag particles should have minimal or no capping, in order to maximize the scattering and the near field effects around them.

Laser ablation (LA) of solid Ag in liquid can meet all the aforementioned requirements. LA in various configurations was used previously for the production of colloidal Ag [13–28]. In particular, most of the relevant, reported works are dealing with colloidal Ag in aqueous solutions [13–23], while studies dealing with organic solvents, such as THF [24], PGMEA [25], various alcohols [13,26,27] and toluene and chloroform [27,28], DMF and THF [29], are less frequent

* Corresponding author. Tel.: +30 6936685104.
*E-mail address:* skasa@physics.auth.gr (S. Kassavetis).

http://dx.doi.org/10.1016/j.apsusc.2014.11.171
0169-4332/

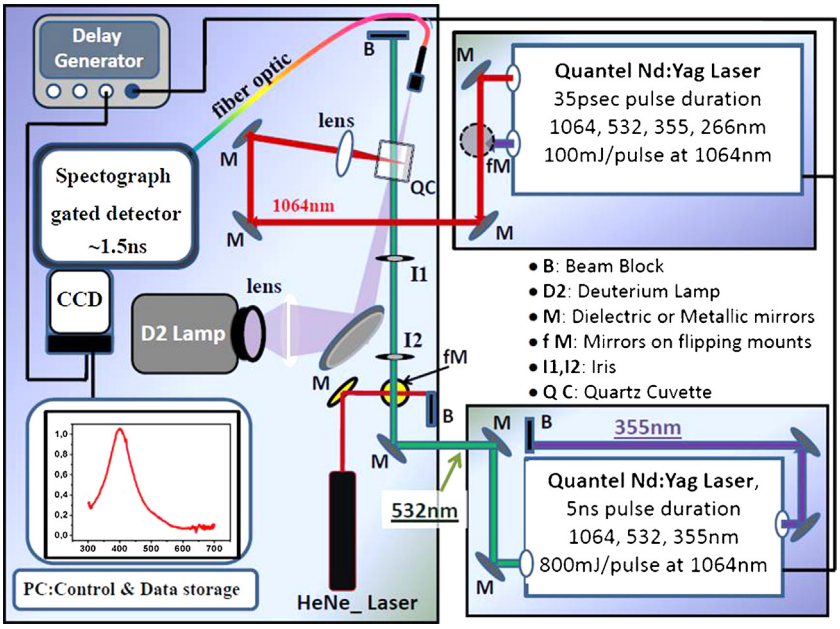


**Fig. 1.** The experimental set up used for laser ablation of the solid target (primary ps laser), laser refinement of particles in the liquid phase (secondary ns laser) and, in situ optical transmittance spectroscopy.

and are focused to ns laser beams [25–29]; when a ns laser beam is used to ablate Ag in organic environment, the produced nanoparticles are exceptionally fine (about 5 nm) [29], therefore, their ability to scatter light is limited. There is still a lack of understanding the effects of pulse duration in the ps–ns range and the wavelengths spanning from infrared (1064 nm) to visible (532 nm) and to UV (355 nm) spectral ranges to the morphology of the produced Ag nanoparticles, as well as the stability of the solvent during the ablation process. The behavior of the solvent under laser irradiation is of particular interest, as it can be the source of various physical effects (e.g. beam confinement and particle cooling [30,31], and it can trigger photochemical reactions, such as photo-isomerization [32] and solvent pyrolysis (in the case of toluene) [33].

In this work, we aim to develop silver NPs plasmonic solutions for application in flexible printed organic solar cells. Therefore we aim to develop Ag NPs bigger than those produced by ns laser beams [29] and with size not exceeding 100 nm, immersed in solutions compatible with the printed solar cells technology, such as water (used as solvent to PEDOT:PSS), and volatile solvents like chloroform and toluene (used as solvents for the active layers, such as P3HT:PCBM). A ps laser beam was used to achieve cold ablation of the silver target and to avoid the stronger thermal effects that a ns beam induces. We study the effects of laser wavelength, fluence, and of the solvent (chloroform or toluene). We also consider the implementation of polyvinylpyrrolidone (PVP) additive, which was proven to be incompatible with the organic solvents and the ps laser beams, because it agglomerates upon laser irradiation.

Finally, we show that the ps laser beams produce bigger Ag nanoparticles, compared to ns beams [29], and the produced nanoparticles can be further refined to a desired size with the use of a secondary ns beam. By this combined, two step process, particles with intermediate sizes, between those produced by the exclusive use of ps or ns laser beams, can be produced.

## 2. Experimental

A home-made optical set up (Fig. 1) was used for the laser ablation process of the solid silver target (primary ps laser), the particle refinement in the liquid phase by laser radiation (secondary ns laser) and in situ and *real-time* optical transmittance measurements.

The laser ablation of the Ag target (polished foil, purity 99.99% by Kurt J. Lesker company) was carried out using the 1064 nm, 532 nm and 355 nm beams of a 35 ps Nd:YAG laser by Quantel (primary laser). The silver target was placed inside a quartz cuvette that was filled with the solvent liquid (chloroform, toluene, or water). The primary laser beam was hard focused on the Ag surface using a fused quartz lens. The silver target was ablated by delivering laser pulses with 10 Hz repetition rate and varying the pulse energy in the range 0.8–17 mJ. The NPs size refinement was made by a secondary nanosecond laser pulse (5 ps), which irradiate and fragment the already developed Ag NPs in out-of-focus mode.

Time resolved transmission spectra are recorded after every single laser shot of the ps laser pulse used for the ablation of the Ag target or the ns pulse used for shaping the resulting nanoparticles in liquid phase. The spectrograph consists of an Andor iStar-CCD camera and an imaging monochromator (Andor-Shamrock 303i). A 150 l/mm grating was used offering a 1 nm spectral resolution and the ability to record in a single shot a region of 400 nm UV–vis spectrum. A D2 lamp is employed as a white light source for the transmission measurements and a couple of lenses are used for collimation and focusing through the liquid sample. Time "slices" of the transmitted D2 lamp spectrum, using gated amplification, in the order of 1 ms have been recorded at a fixed time delay (50 ms) with respect to the ps or the ns laser pulses. The delay time was controlled with sub-nanosecond accuracy via a time-delay-generator (Stanford Research Instruments), "clocked" to the Q-switch process of the ps and ns laser systems.

The Scanning Electron Microscopy (SEM) characterization were carried out in a JEOL JSM-6510LV SEM equipped with $LaB_6$ filament after drop casting and drying of the solution through evaporation of the solvent on aluminum tape; the SEM is equipped with an energy dispersive X-ray detector (EDX) for chemical analysis. Transmission Electron Microscopy (TEM) characterization for selected samples were performed in a JEOL JEM-2100 high resolution transmission electron microscope (HR-TEM) equipped with $LaB_6$ filament after drop casting and drying of the solution through evaporation of the solvent on standard hexagonal 600 mesh copper grids.

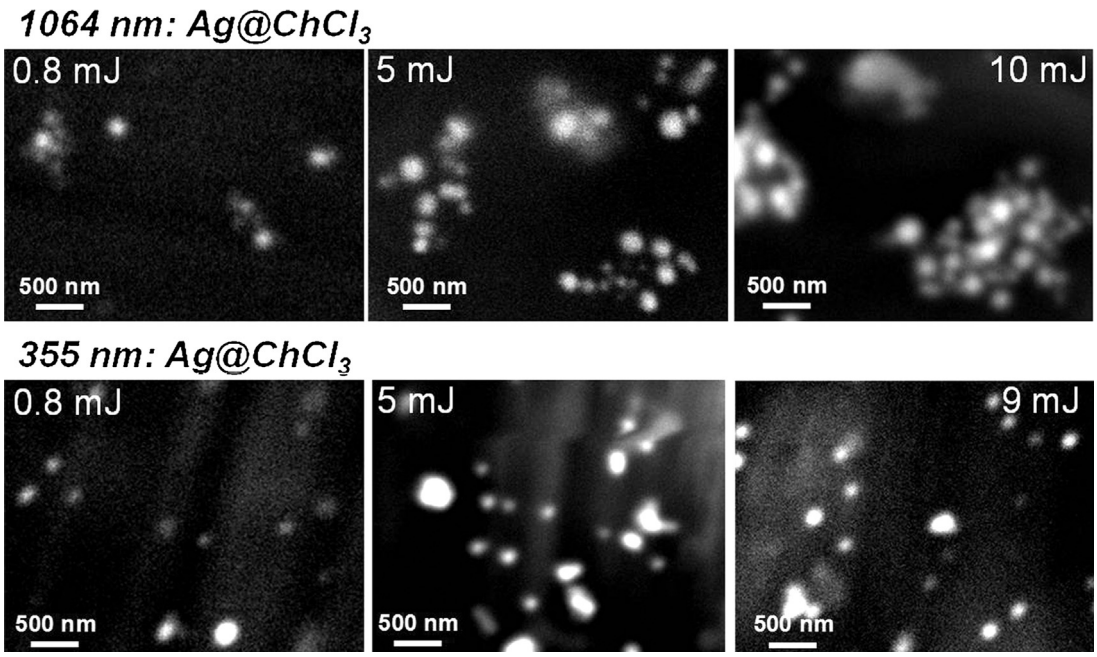


**Fig. 2.** SEM images of the Ag NPs developed in chloroform by laser ablation of a silver target using the 1064 nm and 355 beams of the 35 ps Nd:YAG laser for varying pulse energy.

## 3. Results and discussion

### 3.1. The effect of laser wavelength and fluence

In Fig. 2, SEM images of the Ag NPs that where developed by LA of an Ag target immersed in $CHCl_3$ using the 1064 nm and 355 beams of the 35 ps Nd:YAG laser, are presented. The size and the population of the Ag NPs were found to depend on the laser pulse energy (PE). In details for 1064 nm and PE = 0.8 mJ (Fig. 2 first horizontal line of images), exceptionally low density of Ag NPs was developed and although the Ag NPs were very few, aggregates formation were observed. For $P$ = 5 mJ and $P$ = 10 mJ (Fig. 2, first line, second and third image, respectively) a large population of Ag NPs was developed in various size and shapes. However, no well-defined plasmon response was observed, possibly due to Ag NP aggregation forming micron scale aggregates (Fig. 3a).

In Fig. 2 (second horizontal line of images), the SEM images show the Ag NPs developed in chloroform by using the 355 nm laser beam of the 35 ps Nd:YAG laser and varying the PE from 0.8 to 9 mJ. As in the case of the LA using the 1064 nm beam, the population of the developed Ag NPs considerably increases with increasing the PE, but the formation of larger Ag particles is also observed for $P$ = 4.5 mJ and 9 mJ. The real-time optical absorption spectra (Fig. 3c) shows the presence of an absorption peak at ~565 nm, which corresponds to the Localized Surface Plasmon Resonance (LSPR) of the Ag NPs/$CHCl_3$ solutions, and denotes that: (i) the Ag NPs size distribution is narrow and (ii) the Ag NPs are well isolated. Therefore, LA with the 355 nm beam of the 35 ps laser in low PE, can be used for the development of plasmonic solutions in $CHCl_3$ that contain Ag NPs, which size is compatible with the requirements of the organic and printed photovoltaic devices technology [34].

Moreover the real-time absorption spectra for LA process using the 355 beam shows that the development of plasmonic solution starts during the first minute of the LA process, the LSPR absorption peak further increases and reaches a maximum value after 6 min. Continuation of the LA process did not have any result to this absorption peak and this can be attributed to the scattering of the incident laser beam by the already developed Ag NPs in the solution.

In contrast, the LA of silver in $CHCl_3$ using the 532 nm beam of the 35 ps laser is not promising. For LA using high PE (>10 mJ), Energy Dispersive X-Rays (EDX) revealed that the fine bright features in Fig. 4 are Ag nanoparticles, micro-fragments and

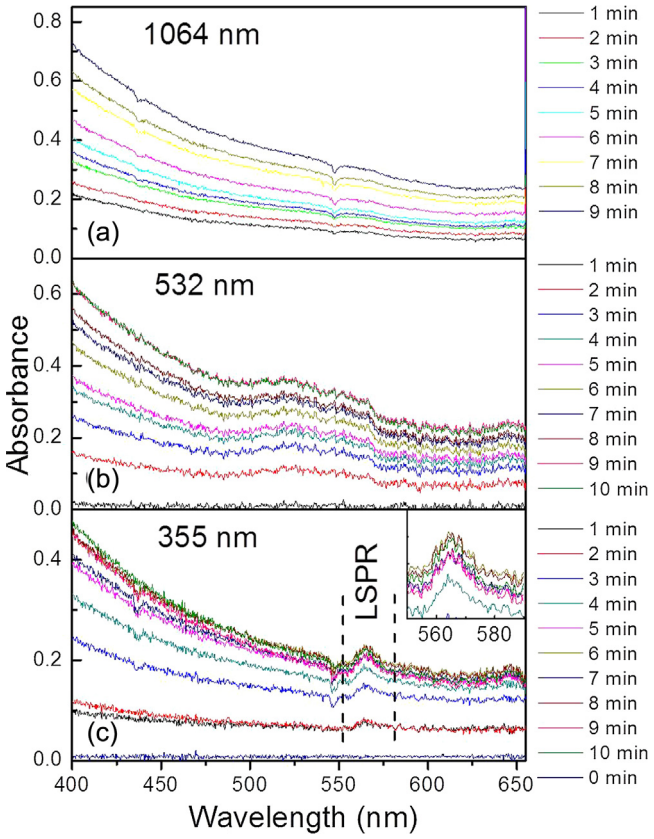


**Fig. 3.** Absorbance spectra for colloidal Ag produced by ps laser ablation in chloroform using three wavelengths (a) 1064 nm, (b) 532, and (c) 355 nm, and various ablation times at 0.8 mJ/pulse. The inset in (c) is a detail of the LSPR feature.

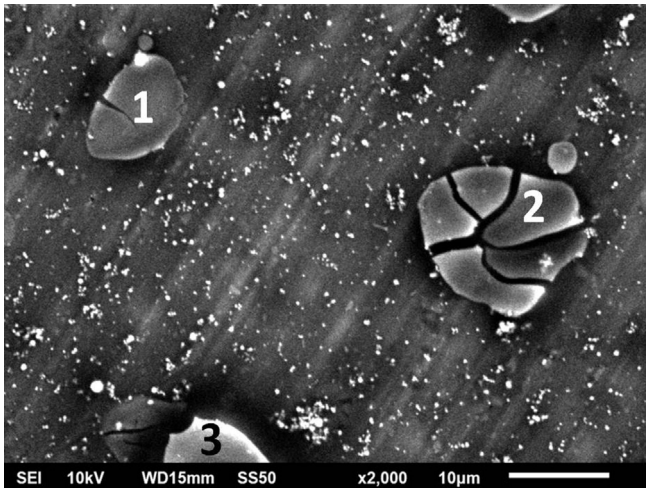


**Fig. 4.** SEM image of the Ag NPs developed in chloroform by laser ablation of a silver target using the 532 nm beam of the 35 ps Nd:YAG laser. The laser power is PE = 10 mJ.

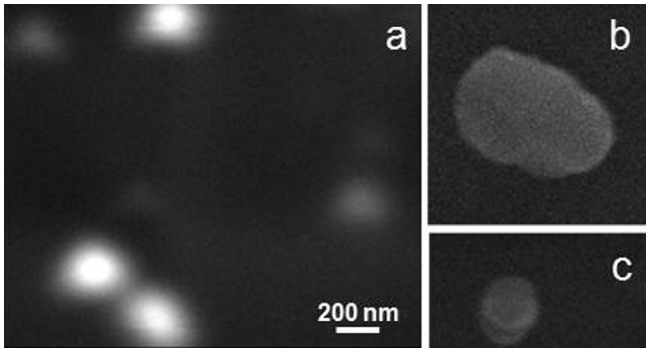


**Fig. 5.** SEM images from (a) Ag@chloroform (355 nm, 10 mJ/cm$^2$), (b) and (c) Ag@toluene (355 nm, 10 mJ/cm$^2$) colloidal plasmonic solutions. The same scale bar applies to all.

aggregates, while the large features (noted as: 1, 2, 3) are organic agglomerates indicating the two-photon photoisomerization of chloroform in agreement to Ref. [32], where the photoisomerization of chloroform by a single 266 nm photon resonant absorption is reported [32]. As a consequence no LSPR was observed in the absorption spectra (Fig. 3b).

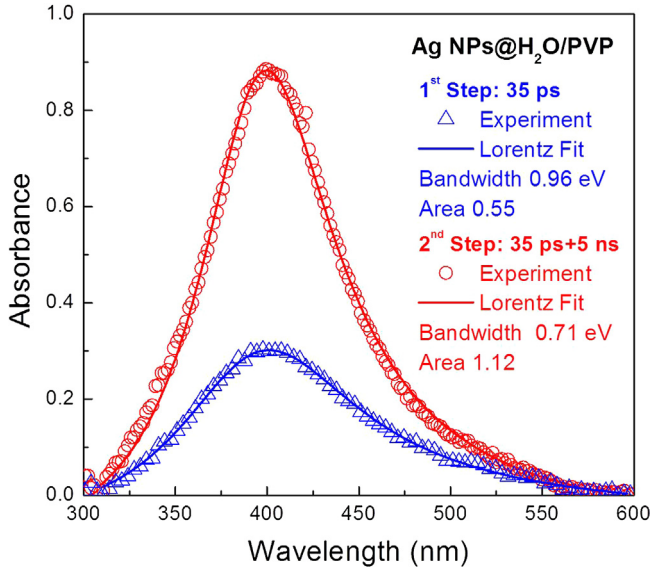


**Fig. 7.** The absorption spectra of the Ag NPs in $H_2O$/PVP before (triangles) and after (circles) the size refinement process using an out-of-focus 5 ns laser beam.

### 3.2. The effect of the organic solvent

Except of the $CHCl_3$, toluene ($C_7H_8$) is also a solvent compatible with the solution processed photoactive polymers technology. In Fig. 5 the SEM images show the Ag NPs developed by LA of silver in toluene solution using the 355 nm beam of the 35 ps laser. Large fragments of Ag together with Ag NPs with size ~200 nm are observed. It should be noted that for the same PE the size of the developed Ag NPs in the $CHCl_3$ is considerably smaller compared to those developed in toluene.

### 3.3. Ag NPs size control – the effect of the PVP additive and the irradiation with a second laser beam

Polyvinylpyrrolidone in CHCl3 and in water was used to prevent the Ag NPs aggregation. The LA ablation of silver immersed in the $CHCl_3$–PVP solution resulted to: (i) no size refinement of the Ag NPs in the case of 0.06 mM PVP in $CHCl_3$ solution and (ii) small size Ag NPs (5–10 nm), not-desirable for the targeted applications (Ag NPs larger than 40 nm are needed [34]), and to the intense agglomeration of the PVP in the case of 3.7 mM PVP in CHCl3 (Fig. 6b).

In water, a quite diverse in size population of Ag NPs is developed. The PVP effectively prevented the formation of aggregates and as a consequence the developed solution shows a plasmonic

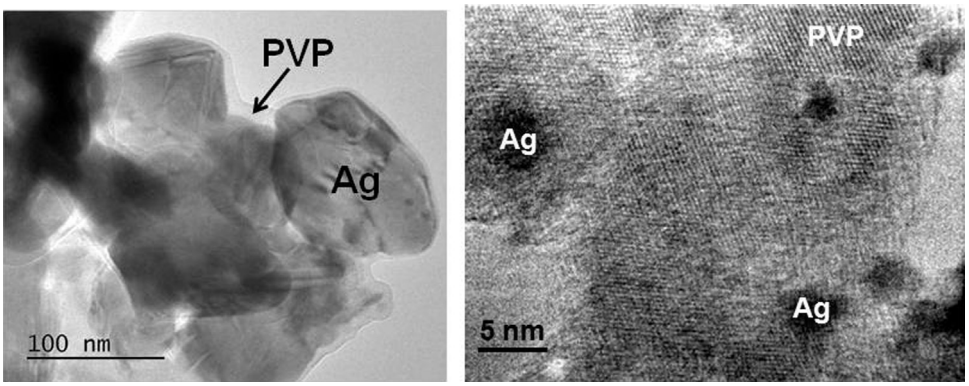


**Fig. 6.** High resolution TEM images show the developed Ag NPs in CHCl3 solution containing (left) 0.06 mM PVP and (right) 3.7 mM PVP. The LA was made using the 355 beam of the 35 ps laser and PE 0.8 mJ/cm$^2$.

peak at the ~400 nm, which is broad and not so intense due to the large variation in the size distribution of the Ag NPs (Fig. 7). In this case the size distribution was successfully altered by the implementation of a secondary laser beam in 355 nm from a 5 ns Nd:YAG laser. The out-of-focus nanosecond laser beam refined the size of the Ag NPs and as a result the plasmonic peak in the absorbance spectra appeared more intense (the absorption increases from 0.3 to 0.9) (Fig. 7). The analysis of the absorption spectra using a Lorentzian oscillator showed that after the irradiation with the second 5 ns laser beam, the absorption peak is less broad, thus the Ag NPs size distribution is narrower, and the under the curve area is double as a result of the Ag NPs population increase due to the successful fragmentation process.

## 4. Conclusions

In summary, the laser ablation development of Ag NPs in organic solvents such as chloroform and toluene using different wavelength beams of the 35 ps Nd:YAG laser was presented. We produced a wide variety of plasmonic colloidal Ag by laser ablation, meeting the requirements of organic and printed electronics. In particular:

1. Formation of Ag nanoparticles of size of the order of 100 nm (much bigger than those produced using a ns beam [29], thus maximizing light scattering) was demonstrated.
2. Increase of the laser fluence results in broader size distribution, mostly due to the formation of bigger fragments that are obstacles for the implementation of these plasmonic colloids to OPV and OLED device fabrication.
3. The 1064 nm beam resulted in agglomerated Ag nanoparticles, while the 532 nm beam of high fluence isomerizes the chloroform and results in a very wide size distribution of Ag nanoparticles; only the 355 nm beam produced well defined LSPR indicating a narrow size distribution with average size about 100 nm.
4. The ablation process stops after about 4500 pulses due to scattering of the incoming laser beam; further irradiation of the liquid phase with a ps beam does not change the LSPR profile and consequently does not affect the particle size distribution. Contrariwise, a ns laser beam irradiating the liquid phase can refine the produced nanoparticles, resulting in a narrower size distribution and in fragmentation of agglomerates. The combination of the two laser beams (ps-ns) can provide nanoparticles of intermediate sizes, i.e. bigger than the ns ablation that provides exceptionally fine particles [29], but smaller than those produce by the exclusive use of the ps laser beam.

## Acknowledgements

This work has been financially supported by the European Union Seventh Framework (FP7/2007-2013) program through the project SMARTONICS, Grant Agreement No. 310229.

The laser ablation experiments and the electron microscopy characterization were realized in the Central Laser Facility and the Central Microscopy Facility, respectively, of the University of Ioannina.

## References

[1] K.R. Catchpole, A. Polman, Opt. Express 16 (2008) 21793.
[2] H.A. Atwater, A. Polman, Nat. Mater. 9 (2010) 205–213.
[3] V.E. Ferry, M.A. Verschuuren, H.B.T. Li, E. Verhagen, R.J. Walters, R.E.I. Schropp, H.A. Atwater, A. Polman, Opt. Express 18 (2010) A237.
[4] J.-L. Wu, F.-C. Chen, Y.-S. Hsiao, F.-C. Chien, P. Chen, C.-H. Kuo, M.H. Huang, C.-S. Hsu, ACS Nano 5 (2011) 959–967.
[5] G.D. Spyropoulos, M. Stylianakis, E. Stratakis, E. Kymakis, Phot. Nanostr. Fund. Appl. 9 (2011) 184–189.
[6] N. Kalfagiannis, P.G. Karagiannidis, C. Pitsalidis, N.T. Panagiotopoulos, C. Gravalidis, S. Kassavetis, P. Patsalas, S. Logothetidis, Solar Energy Mater. Solar Cells 104 (2012) 165–174.
[7] Q. Gan, F.J. Bartoli, Z.H. Kafafi, Adv. Mater. 25 (2013) 2385–2396.
[8] M.J. Beliatis, S.J. Henley, S. Han, K. Gandhi, A.A.D.T. Adikaari, E. Stratakis, E. Kymakis, S.R.P. Silva, Phys. Chem. Chem. Phys. 15 (2013) 8237–8244.
[9] E. Stratakis, E. Kymakis, Mater. Today 16 (2013) 133–146.
[10] A. Fujiki, T. Uemura, N. Zettsu, M. Akai-Kasaya, A. Saito, Y. Kuwahara, Appl. Phys. Lett. 96 (2010) 043307.
[11] X. Gu, T. Qiu, W. Zhang, P.K. Chu, Nanoscale Res. Lett. 6 (2011) 199.
[12] F. Liu, J.-M. Nunzi, Proc. SPIE 8424 (2012) 84243E.
[13] N. Bärsch, J. Jakobi, S. Weiler, S. Barcikowski, Nanotechnology 20 (2009) 445603.
[14] T. Tsuji, D.-H. Thang, Y. Okazaki, M. Nakanishi, Y. Tsuboi, M. Tsuji, Appl. Surf. Sci. 254 (2008) 5224–5230.
[15] A.S. Nikolov, R.G. Nikov, I.G. Dimitrov, N.N. Nedyalkov, P.A. Atanasov, M.T. Alexandrov, D.B. Karashanova, Appl. Surf. Sci. 280 (2013) 55–59.
[16] G.K. Podagatlapalli, S. Hamad, S.P. Tewari, S. Sreedhar, M.D. Prasad, S.V. Rao, J. Appl. Phys. 113 (2013) 073106.
[17] A.-M. Dallaire, D. Rioux, A. Rachkov, S. Patskovsky, M. Meunier, J. Phys. Chem. C116 (2012) 11370–11377.
[18] E. Messina, L. D'Urso, E. Fazio, C. Satriano, M.G. Donato, C. D'Andrea, O.M. Marago, P.G. Gucciardi, G. Compagnini, F. Neri, J. Quant. Spectr. Rad. Transf. 113 (2012) 2490–2498.
[19] R.G. Nikov, A.S. Nikolov, N.N. Nedyalkov, I.G. Dimitrov, P.A. Atanasov, M.T. Alexandrov, Appl. Surf. Sci. 258 (2012) 9318–9322.
[20] E. Akman, B. Genc-Oztoprak, M. Gunes, E. Kacar, A. Demir, Photon. Nanostr. Fund. Appl. 9 (2011) 276–286.
[21] K. Siskova, B. Vlckova, P.-Y. Turpin, A. Thorel, M. Prochazka, J. Phys. Chem. C115 (2011) 5404–5412.
[22] A. Pyatenko, K. Shimokawa, M. Yamaguchi, O. Nishimura, M. Suzuki, Appl. Phys. A 79 (2004) 803–806.
[23] G.A. Shafeev, E. Freysz, F. Bozon-Verduraz, Appl. Phys. A 78 (2004) 307–309.
[24] A. Schwenke, P. Wagener, S. Nolte, S. Barcikowski, Appl. Phys. A104 (2011) 77–82.
[25] H. Shi, C. Wang, Y. Zhou, K. Jin, G. Yang, J. Nanosci. Nanotechnol. 12 (2012) 1–7.
[26] D. Werner, S. Hashimoto, T. Tomita, S. Matsuo, Y. Makita, J. Phys. Chem. C112 (2008) 1321–1329.
[27] M. Kalyva, S. Kumar, R. Brescia, S. Petroni, C. La Tegola, G. Bertoni, M. De Vittorio, R. Cingolani, A. Athanassiou, Nanotechnology 24 (2013) 035707.
[28] A.M. Brito-Silva, L.A. Gomez, C.B. de Araujo, A. Galembeck, J. Nanomater. (2010) (art. no 142897).
[29] V. Amendola, S. Polizzi, M. Meneghetti, Langmuir 23 (2007) 6766.
[30] T. Tsuji, T. Kakita, M. Tsuji, Appl. Surf. Sci. 206 (2003) 314.
[31] A.V. Kabashin, M. Meunier, C. Kingston, J.H.T. Luong, J. Phys. Chem. B107 (2003) 4527.
[32] F. Abou-Chahine, T.J. Preston, G.T. Dunning, A.J. Orr-Ewing, G.M. Greetham, I.P. Clark, M. Towrie, S.A. Reid, J. Phys. Chem. A117 (2013) 13388.
[33] V. Amendola, S. Polizzi, M. Meneghetti, Sci. Adv. Mater. 4 (2012) 1.
[34] S.-W. Baek, J. Noh, C.-H. Lee, B.S. Kim, M.-K. Seo, J.-Y. Lee, Sci. Rep. 3 (2013) 1726.